EBioMedicine 56 (2020) 102819

Contents lists available at ScienceDirect

EBioMedicine

journal homepage: www.elsevier.com/locate/ebiom

Research paper

A novel rabies vaccine based on infectious propagating particles derived from hybrid VEEV-Rabies replicon

Ya-Nan Zhang[a,c,1], Chen Chen[b,d,1], Cheng-Lin Deng[a], Cheng-guang Zhang[b,d], Na Li[a,c], Zhen Wang[e], Ling Zhao[b,d,**], Bo Zhang[a,e,*]

[a] Key Laboratory of Special Pathogens and Biosafety, Wuhan Institute of Virology, Center for Biosafety Mega-Science, Chinese Academy of Sciences, Wuhan, China
[b] State Key Laboratory of Agricultural Microbiology, Huazhong Agricultural University, Wuhan, Hubei 430070, China
[c] University of Chinese Academy of Sciences, Beijing 100049, China
[d] College of Veterinary Medicine, Huazhong Agricultural University, Wuhan, Hubei 430070, China
[e] Drug Discovery Center for Infectious Disease, Nankai University, Tianjin 300350, People's Republic of China

ARTICLE INFO

Article History:
Received 27 February 2020
Revised 11 May 2020
Accepted 14 May 2020
Available online xxx

Key words:
Rabies
VEEV
Live attenuated vaccine
Glycoprotein

ABSTRACT

Background: Live attenuated vaccines (LAVs) can mimic natural infection and have advantages to stimulate a robust and sustained immune response as well as to confer long-term protection. However, safety concerns is one of the major obstacles for LAVs development. In an effort to achieve the optimal balance between immunogenicity and safety, researchers currently have taken different strategies for the development of LAVs.

Methods: We constructed a novel infectious self-propagating hybrid replicon particle (PRP), VEEV-RABV-G, through replacing the entire structural proteins of the Venezuelan equine encephalitis virus (VEEV) with the glycoprotein of rabies virus (RABV-G) as the single structural protein. We evaluated the potential of VEEV-RABV-G as a safe live attenuated vaccine in mice model.

Findings: We found that VEEV-RABV-G could self-propagate efficiently in cell culture and induce a robust humoral immunity and provide protection against virulent RABV challenge in immunized mice. Remarkably, VEEV-RABV-G is highly attenuated in both adult and sucking mice, causing much weaker inflammatory and apoptotic effects in the brains of infected adult mice and significantly lower weight loss and morbidity compared with the commonly used RABV-derived LAVs.

Interpretation: This study reveals the feasibility of developing novel rabies vaccines based on the self-replicating PRPs.

Funding: This work was supported by the National Key Research and Development Program of China (2016YFD0500400).

1. Introduction

Rabies virus (RABV) is neurotropic, enveloped, single-stranded, negative-sense RNA virus. It belongs to the *Lyssavirus* genus, *Rhabdoviridae* family. RABV infection causes fatal encephalitis known as rabies in the mammals [1]. Despite the first successful human immunization against rabies reported more than 100 years ago, nowadays rabies is still responsible for 59,000 - 61,000 human deaths annually around the world [2-4]. Currently, the most widely used rabies vaccines, such as RabAvert and Rabipur, are all inactivated vaccines [5, 6]. As the inactivated vaccines fail to induce strong immunity to provide long-term protection against RABV infection, the vaccine recipients have to receive four to five shots over time to acquire ideal immunity protection. Besides inconvenience and discomfort to recipients, it increases the cost of vaccination. Such high cost of rabies vaccines greatly limits their accessibility, especially in the low- and middle-income countries where the rabies is endemic, and consequently, results in poor control of this disease. Therefore, it is necessary to develop new efficacious, convenient, affordable rabies vaccines to prevent RABV infection.

Unlike inactivated vaccines, live attenuated vaccines (LAVs) mimic natural infection, and often a single dose is enough to induce a robust and sustained immune response and provide long-term protection

* Corresponding author: Bo Zhang, PhD, (Lead contact) Key Laboratory of Special Pathogens and Biosafety, Center for Emerging Infectious Diseases, Wuhan Institute of Virology, Chinese Academy of Sciences, Wuhan, China
** Ling Zhao, PhD, State Key Laboratory of Agricultural Microbiology, College of Veterinary Medicine, Huazhong Agricultural University, Wuhan, China.
E-mail addresses: zling604@yahoo.com (L. Zhao), zhangbo@wh.iov.cn (B. Zhang).
[1] These authors contributed equally to this work.

https://doi.org/10.1016/j.ebiom.2020.102819

RESEARCH IN CONTEXT

Evidence before this study

Rabies virus (RABV) infection causes fatal encephalitis known as rabies in the mammals. Currently, both inactivated and live attenuated vaccines are available against RABV. Inactivated vaccines require repeated immunization to obtain ideal immunity protection. One dose of live attenuated vaccines is usually enough to provide robust and sustained immune responses, but safety is the major concern for this type of vaccines. New strategy is required for developing rabies vaccines with satisfactory safety and efficacy.

Added value of this study

The novel infectious propagating replicon particle (PRP), VEEV-RABV-G, was developed as a live attenuated rabies vaccine in this study. VEEV-RABV-G was infectious and propagated efficiently in cell culture with VEEV replicon expressing the single structural protein, RABV-G. VEEV-RABV-G particles were highly attenuated and provided strong protective immunity against lethal RABV challenge.

Implications of all the available evidence

The satisfactory safety and immunogenicity make VEEV-RABV-G a promising LAV candidate against RABV infection for human and domestic animal use.

against virus infection. Development of rabies LAVs represents a promising approach to improve the efficacy of rabies prevention and reduce vaccination costs [7-9]. So far, in spite of increasing utilization of LAVs for oral rabies vaccination of wildlife (eg. raccoons, foxes and coyotes) [1], the rabies LAVs for pets and human use are still lacking. All the current rabies LAVs used for wildlife, including SAD Bern, SAD B19 and SAG2, are generated through repeated passage of the SAD (Street Alabama Dufferin) strain in cell culture, thus their possible reversion to virulence may become the critical limitation for their further utilization in pets, especially in human. Fortunately, the reverse genetic techniques offer an alternative solution to develop safe and effective rabies LAVs by using a variety of relatively safe viral vectors. The genome of RABV encodes five structural proteins defined as nucleocapsid protein (N), phosphoprotein (P), matrix protein (M), glycoprotein (G), and large polymerase (L) [10, 11]. Among these, RABV glycoprotein (RABV-G), the only surface-exposed protein on virions, has been demonstrated to be the major viral component responsible for the induction of host antibody response, therefore serving as an important immunogen of rabies vaccines [12, 13]. Researchers have developed various constructs expressing RABV-G protein in the context of poxviruses [12, 14, 15], paramyxoviruses [13, 16] and adenoviruses vectors [17, 18], which could induce a robust humoral immune response against RABV.

In this study, a novel infectious propagating replicon particle (PRP), VEEV-RABV-G, was developed as a live attenuated rabies vaccine through replacement of the structural genes of Venezuelan equine encephalitis virus (VEEV) with RABV-G. The glycoprotein of RABV enables the efficient packaging of the chimeric replicon RNA into infectious particles which could self-propagate in cell culture to high titers. VEEV-RABV-G particles were highly attenuated in adult and suckling mice and could induce potent humoral immune responses even at a relatively low dose. Mice vaccinated with VEEV-RABV-G via intramuscular (i.m.) were protected from a lethal RABV challenge through intracranial (i.c.) route. The atisfactory safety and immunogenicity makes VEEV-RABV-G as a promising safe LAV candidate against RABV infection.

2. Materials and Methods

2.1. Cells, viruses and animals

BHK-21 cells, BSR cells (a BHK-21 clone) and B7GG cells (a BHK-21 clone expressing T7 RNA polymerase, rabies virus G and histone2B-tagged GFP) were cultured in Dulbecco's modified Eagle's medium (DMEM; Thermo Fisher Scientific Inc., Waltham, MA, USA) containing 10% fetal bovine serum (FBS, Fisher Scientific Inc.) and 100 U/mL of penicillin and 100 μg/mL of streptomycin at 37°C with 5% CO_2 [19]. RABV vaccine strains including LBNAR and LBNSE were recovered using B7GG cells, which were propagated and amplified in BSR cells, as described previously [20]. LBNAR was derived from SAD L16 cDNA clone, and LBNSE was constructed from LBNAR with two mutants in the G protein at amino acid position 194 and 333 [21]. RABV virulent strains including CVS-24 (challenge virus standard strain 24) and DRV-Mexico (A dog-derived RABV wild-type strain) were applied in challenge test after vaccination. CVS-24 is a mouse-adapted laboratory strain, and DRV-Mexico strain was isolated from a human patient and propagated in the brains of newborn mice [22, 23]. Female ICR mice and Balb/c mice at the age of 6-8 weeks as well as 3-5 days sucking KM (Chinese Kun Ming) mice were obtained from the Center for Disease Control and Prevention of Hubei Province, P.R. China. All mice were housed in individually ventilated cages in the Animal Facility at Huazhong Agricultural University (HZAU) located in Wuhan City, Hubei Province, P.R. China.

2.2. Antibodies

Anti-RABV glycoprotein mAb (clone no. 1C5, cat. no. 135206) for indirect immunofluorescence assay (IFA) was purchased from Abcam Inc. (Cambridge, Cambs, UK). Anti-RABV glycoprotein mAb (clone no. 2B10) for western-blot (WB) assay were provided by by Dr. Ling Zhao at HZAU. For IHC, anti-mouse CD45 mAb (cat. no. GB11066) and anti-mouse caspase-3 pAb (cat. no. GB11009) were purchased from Servicebio technology Co., Ltd. (Wuhan, CHN) FITC or HRP conjugated goat anti-mouse/rabbit IgG were purchased from Proteintech Group Inc. (Chicago, IL, USA). These direct-labelled antibodies against special cell markers were used to analyze immune cells by flow cytometry [8, 20]. FITC anti-mouse CD4 antibody (cat. no. 100510), APC anti-mouse CD185 (CXCR5) antibody (cat. no. 145506) and PE anti-mouse CD279 (PD-1) antibody (cat. no. 135206) were utilized to analyze the numbers of Tfh cells. FITC anti-mouse CD20 antibody (cat. no. 150408), Alexa Flour 647 anti-mouse GL7 antibody (cat. no. 144605), and PE anti-mouse CD95 antibody (cat. no.152607) were applied to analyze the numbers of GC B cells. FITC anti-mouse/human CD45R/B220 antibody (cat. no. 103206), APC anti-mouse CD138 (Syndecan-1) antibody (cat. no. 142506) and PE anti-mouse CD38 antibody (cat. no. 102708) were used to analyze the numbers of PCs. All of these antibodies were purchased from BioLegend, Inc. (San Diego, CA, USA) or BD Bioscience, Inc. (Franklin Lakes, NJ, USA).

2.3. Construction and recovery of the VEEV-RABV-G chimera

VEEV-RABV-G plasmid was constructed using standard recombinant DNA techniques. The complete glycoprotein sequence of LBNAR was amplified using LBNAR infectious clone as the template and cloned into an alphavirus VEEV replicon expression vector at unique AscI and PacI site. The resulting plasmid VEEV-RABV-G was verified by DNA sequencing. The cDNA plasmid was subjected to sequential *Not*I linearization and *in vitro* transcription using mMESSENGER mMACHINE T7 Kit (cat. no. AMB13445, Ambion, Fisher Scientific Inc.) following the manufacturer's protocols. The yield and integrity of

RNA transcripts were analyzed by gel electrophoresis under non-denaturing conditions. RNA transcripts (1 μg) were transfected into BHK-21 cells with DMRIE-C (cat. no. 10459014, Invitrogen, Fisher Scientific Inc.) according to the manufacturer's instructions. Supernatants were then collected at 5 days post transfection when typical CPE was observed and aliquoted and stored at −80°C for the following experiments.

2.4. Virus titration and growth curves

VEEV-RABV-G titer was determined by standard plaque assay on BHK-21 cells as described previously [24]. Briefly, BHK-21 cells in 24-well plates were infected with a 10-fold serial dilution of viruses. The plates were incubated at 37°C for 1 h before the layer of 1% methylcellulose in DMEM containing 2% FBS was added. After further incubation at 37°C for 5 days, the cells were fixed with 3.7% formaldehyde and stained with 1% crystal violet to visualize the plaques. RABV titer was determined by fluorescent plaque assay on BSR cells. In brief, RABVs were 10-fold serially diluted and added into 24-well plates containing sub-confluent monolayer of BSR cells. After incubation for 1 h at 37°C, the culture medium was discarded, and the adherent cells were washed 3 times before the layer of 1% methylcellulose in DMEM containing 2% FBS was added. After incubation for 2 days at 37°C, the adherent cells were washed and fixed with 80% ice-cold acetone at −20°C for 1 h. After 3 washes with PBS, the cells were stained with FITC-conjugated anti-RABV N protein antibodies for 1 h at 37°C. After 3 washes with PBS, antigen-positive fluorescent foci on the cells were counted under an Olympus IX51 fluorescence microscope (Olympus, Tokyo, JPN). Growth curves of VEEV-RABV-G in BHK-21 cells were performed in a 35 mm dish at a multiplicity of infection (MOI) of 0.01. Cell supernatants were collected at successive 24 h intervals post-infection. Viral titers were then quantitated by plaque assay on BHK-21 cells as described above.

2.5. Indirect immunofluorescence assay (IFA)

BHK-21 cells were seeded into 35 mm dishes containing coverslips and transfected with the VEEV-RABV-G genomic RNA or infected with the VEEV-RABV-G virus at an MOI of 0.01. At indicated time points, the coverslips containing transfected or infected cells were collected, washed with PBS and fixed with cold (-20°C) 5% acetic acid in acetone for 15 min at room temperature. After washing with PBS three times, the fixed cells were reacted with RABV-G murine monoclonal antibodies diluted in PBS (1:500) for 1 h. The cells were washed three times with PBS and further incubated with goat anti-mouse IgG antibodies conjugated with FITC (1:125 dilution in PBS) at room temperature for 1 hour. After which the cells were washed three times with PBS following mounted with 90% glycerol and examined under a fluorescent microscope. The fluorescent images were taken at 200 × magnification with a Nikon upright fluorescence microscope (Nikon, Tokyo, Japan).

2.6. Western blotting analysis

BHK-21 cells were infected with LBNAR or VEEV-RABV-G at an MOI of 0.1. At 48 hpi (LBNAR) or 72 hpi (VEEV-RABV-G), the cells were lysed with RIPA buffer (Beyotime, China).Proteins were separated by 12% SDS-PAGE and then electro-transferred onto the 0.2 μm of polyvinylidene fluoride (PVDF) membrane (Merck Millipore, Darmstadt, GER) followed by blocking with 5% skim milk in TBST (50 mM Tris-HCl, 150mM NaCl, 0.1% Tween 20, pH 7.4) for 1 h at room temperature. The blocked membranes were then incubated with primary antibody of anti-RABV glycoprotein mAb (clone no. 2B10) with 1:1000 dilution at room temperature for another 1 h. After washing three times with TBST, the membranes were incubated with horseradish peroxidase (HRP) conjugated secondary goat anti-mouse (Proteintech Group Inc.) at room temperature for 1 h, followed by washing three times with TBST. The protein bands were visualized with a chemiluminescent HRP -conjugated antibody detection reagent (Merck Millipore).

2.7. Purification of VEEV-RABV-G virions

BHK-21 cells were infected with VEEV-RABV-G at an MOI of 0.01 and incubated for 96 h at 37°. The medium was reclaimed through sequential centrifugation at 400 g for 10 min and 5,000 g for 20 min at 4°C to remove cells and cell debris. After filtration through a 0.22 μm filter (Merck Millipore), the clarified supernatants were concentrated with polyethylene glycol-8000 (PEG 8000) precipitation at a final concentration of 8% at 4°C overnight. After centrifugation at 14,000 g for 1 h at 4°C, the pellet was gently resuspended in 1mL PBS and then layered onto 4.5 mL of 10% sucrose in PBS and centrifuged at 38,000 rpm for 1 h in a Beckman SW41 rotor. The pellet was resuspended in 100 μL of PBS. VEEV-RABV-G virions were grown and purified in parallel to provide markers for SDS-PAGE gel electrophoresis.

2.8. Thin-section electron microscopy (TEM)

BHK-21 cells monolayers were infected with LBNAR or VEEV-RABV-G at an MOI of 0.01. At 72 hpi, both infected BHK-21 cells were pre-fixed with 2.5% glutaraldehyde at room temperature for 2 h before scraped and pelleted by centrifugation at 400 g for 10 min. Following rinsed with 0.1 M PBS, cells were post-fixed with 1% O_SO_4 at least 2 h at 4°C. All pellets were dehydrated stepwise in a graded series of ethanol and embedded in Epon-812. Ultrathin sections were cut on Leica EM UC7 ultramicrotome (Leica Microsystems, Wetzlar, GER), double-stained with uranyl acetate and lead citrate. The grids containing ultra-thin sections were examined with an Tecnai G^2 20 TWIN microscope (FEI,USA) operated at 200 kV.

2.9. Studies of pathogenicity, immunization and protection

The pathogenicity of VEEV-RABV-G was evaluated and compared with both LBNSE and LBNAR. Groups of adult ICR mice (6-week old) were i.c. mock (DMEM) infected or infected with VEEV-RABV-G, LBNSE and LBNAR at a dose of 5×10^3 FFU in a volume of 25 μl, respectively. Groups of sucking KM mice (3-5 days old) were i.c. mock (DMEM) inoculated or inoculated with 2×10^3 FFU of LBNSE and VEEV-RABV-G in a volume of 10 μl, respectively. Mice body weight and survival data were recorded daily for 15 days after infection, and the mice that displayed deep coma or lost more than 25% of their starting body weight were humanely euthanized with CO_2.

The immunogenicity and protection efficacy of VEEV-RABV-G were also assessed and compared with LBNAR. Groups of adult ICR mice (6-8 weeks old) were i.m. immunized with a high dose (2×10^5 FFU) or a low dose (2×10^4 FFU) of LBNAR and VEEV-RABV-G, respectively. Sera from immunized mice were collected at 1-week intervals over six weeks. For the high-dose immunized groups, at six weeks post-immunization, they received a challenge of $50 \times LD_{50}$ CVS-24 strain by i.c. route. For the los-dose immunized groups, at eight weeks post-immunization, they were challenged with $100 \times LD_{50}$ of DRV-Mexico strain via i.m. route. After challenge, all mice were observed continuously for 21 days, and the mice that displayed deep coma or lost more than 25% of their starting body weight were humanely euthanized with CO_2.

2.10. Hematoxylin and Eosin (H&E)staining and Immunohistochemistry

In order to study the histological changes in adult mice, groups of adult ICR mice (6-week old) were i.c. mock (DMEM) infected or infected with 5×10^3 FFU of VEEV-RABV-G, LBNSE and LBNAR in a volume of 25 μl, respectively. At 9 days post infection (d.p.i.), all

infected mice were anesthetized and perfused with phosphate-buffered saline (PBS, pH 7.4) followed by 4% paraformaldehyde. Then, brains were removed and post-fixed with the same fixative for 3 days. Fixed brains were embedded in paraffin and then sagittally sectioned at 4-μm thickness on a microtome, and mounted on APS-coated slides. For H&E stain, sagittal sections were deparaffinized and stained with H&E (HE, Merck, Darmstadt, Germany). For CD45 and caspase 3 staining, sections were respectively incubated with anti-mouse CD45 mAb (1:3000) or anti-mouse caspase 3 pAb (1:500) in PBS containing 4% goat serum and 0.2% TritonX-100, followed by incubations with an HRP-conjugated goat anti-mouse (or rabbit) antibodies. Positive cells developed by DAB reagent were brown-yellow, and nucleus stained with hematoxylin were blue.

2.11. Measurement of RABV-specific VNA titers

Virus-neutralizing antibody (VNA) titers were measured using the fluorescent-antibody virus neutralization (FAVN) test, as described previously [1, 8, 9]. Briefly, the serum of mice was isolated and inactivated for 30 min at 56°C, and then, 100 μl of DMEM was added into a 96-well plate, and 50 μL of inactivated serum was added into the first column and serially diluted at three-fold. After dilution, the serum was neutralized with 50 μL of CVS-11 (100 FFU per well) at 37°C for 1 h. After neutralization, 100 μl of BSR cells (2×10^4 cells per well) were added into the neutralized medium in the 96-well plates. After incubation for 72 h at 37°C in 5% CO_2, BSR cells were then fixed with 80% ice-cold acetone at −20°C for 30 min and stained with FITC-conjugated RABV N mAb at 37°C for 1 h. Fluorescence was observed under an Olympus IX51 fluorescence microscope (Olympus, Tokyo, JPN). The fluorescence values of measured serum were compared with those of a reference serum obtained from the National Institute for Biological Standards and Control, Hertfordshire, UK, and the results were normalized and quantified in international units per ml.

2.12. Flow cytometry and ELISpot Assay

Immune cells in the inguinal lymph nodes (LNs) and bone marrow (BM) were analyzed by flow cytometry. Briefly, the LNs and BM of mice were collected, and solid tissues were carefully ground in pre-cooled PBS (pH 7.4). The cells were resuspended in PBS containing 0.2% BSA, w/v, and transferred into a tube through a 40-μm nylon filter, then centrifuged, and washed with PBS containing 0.2% BSA. Red blood cells were removed by lysis buffer (cat. no. 555899, BD Biosciences Inc., Franklin Lakes, NJ, USA). After washing twice, the single suspended cells in PBS containing 0.2% BSA were counted. 1×10^6 cells were stained with fluorescence-labeled antibodies. After incubation for 30 min at 4°C, cells were washed twice with PBS (containing 0.2% BSA). Finally, stained cells were analyzed using BD FACSVerse (BD Biosciences Inc.).

ELISpot assay was performed to assess the generation of these antibody secreting cells (ASCs) in the inguinal LNs. Briefly, multi-screen-HA ELISpot plates (Millipore, MA, USA) were coated with purified RABV virions and incubated for 16 h at 4°C. Coated plates were washed and blocked with RPMI 1640 supplemented with 10% FBS for 2 h in 37°C. Cell suspensions prepared from inguinal LNs were transferred to the blocked ELISpot plates and put into 37°C incubator for 24 h. Then the cells in ELISpot plates were incubated sequentially with biotin conjugated mouse IgG antibody (Bethyl Laboratories, TX,

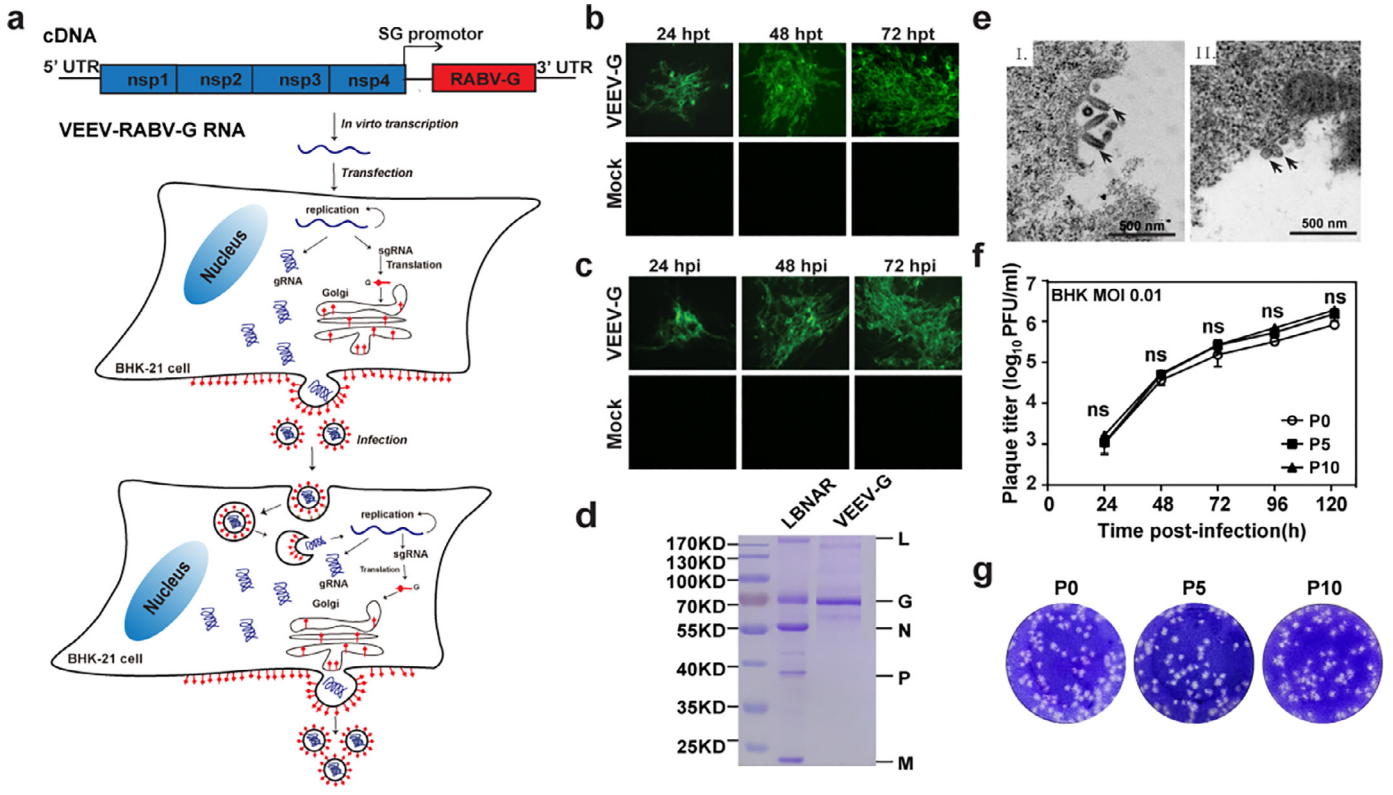

Fig. 1. Construction and characterization of VEEV-RABV-G. (a) Experimental rationale. The diagram outlines the production and infection prosperity of VEEV-RABV-G.(b) Immunostaining of VEEV-RABV-G RNA-transfected BHK-21 cells with RABV-G antibodies at the indicated times post-transfection. (c) IFA of VEEV-RABV-G-infected BHK-21 cells. BHK-21 cells were infected with the supernatants harvested from VEEV-RABV-G genomic RNA-transfected BHK-21 at 72 hpt. At the indicated time points, the expression of RABV-G protein was analyzed by IFA. (d) SDS-PAGE analysis of purified VEEV-RABV-G virions. Purified RABV virions or VEEV-RABV-G PRPs (1 μg of protein each) were fractionated by 12% SDS-PAGE gel and the protein bands were visualized with coomassie staining. The positions and molecular weights of the RABV structural proteins N, P, M, G, and L are indicated. (e) Thin-section TEM of cells infected with RABV vaccine strain LBNAR (I) or VEEV-RABV-G PRPs (II). Scale bars for all TEM images are shown as indicated. (f) Comparison of growth kinetics of P0 and P10 VEEV-RABV-G viruses. The viral growth curves were conducted at an MOI = 0.01. Three independent experiments were performed in duplicate, and the representative data were presented. (g) Plaque morphology comparison between P0, P5 and P10 passage of VEEV-RABV-G in BHK-21 cells.

USA) and streptavidin-alkaline phosphatase (Mabtech, Stockholm, Sweden), finally were colored using BCIP/NBT-plus (Mabtech, Stockholm, Sweden) [25].

2.13. Statistical analysis

We used GraphPad Prism 6.0 (GraphPad Software, Inc., San Diego, CA) to perform the statistical analysis. Results are expressed as mean ± standard deviation (SD) or mean ± standard error of the mean (SEM). For analyses of survival data, the log-rank test was used. The significance of the differences between groups was evaluated by one-way analysis of variance followed by Tukey's post hoc test or student's *t*-test. *p* values of ≤ 0.05 (*), ≤ 0.01 (**), and ≤ 0.001 (***) between different groups were regarded as significant, highly significant, and very highly significant, respectively.

2.14. Ethics statement

All the mice used in this study were maintained in compliance with the recommendations in the Regulations for the Administration of Affairs Concerning Experimental Animals made by the Ministry of Science and Technology of China. The experiments were carried with the protocols approved by the Scientific Ethics Committee of Huazhong Agricultural University (permit number: HZAUMO-2018-040).

3. Results

3.1. VEEV-RABV-G can self-replicate in cells

Firstly, we examined whether VEEV replicon derived PRPs displaying RABV-G on the surface could replicate. As shown in Fig. 1a, RABV-G gene under the control of 26S subgenomic promoter was inserted in place of the genes encoding the VEEV structural proteins. The chimeric VEEV-derived replicon RNA (VEEV-RABV-G) was transfected into BHK-21 cells. Then, the expression of RABV-G was confirmed by immunofluorescence assay (IFA). Time-dependent accumulation of IFA-positive cells was observed from 24 to 72 h post-transfection (hpt), which showed the successful recovery of the production and spreading of the infectious particles of VEEV-RABV-G (Fig. 1b). To further analyze the infectivity of VEEV-RABV-G, the culture media collected from the transfected cells at 72 hpt were used to infect naïve BHK-21 cells. As shown in Fig. 1c, the infected BHK-21 cells produced IFA positive cells at the indicated time points post-infection, confirming the infectivity of VEEV-RABV-G in BHK-21 cells. Meanwhile, Western blotting assay was carried out to evaluate RABV-G protein expression in VEEV-RABV-G infected cells. RABV-G produced by VEEV-RABV-G migrated at the same position in SDS-PAGE gels as RABV vaccine strain, LBNAR did (Fig. 2a). VEEV-RABV-G replicated efficiently with a peak titer of 10^6 FFU/ml at 120 hpi at a multiplicity of infection (MOI) of 0.01 (Fig. 1f) and produced plaques in BHK-21 cells (Fig. 1g). Overall, our results showed that VEEV-RABV-G could be rescued and was infectious in BHK-21 cells.

To further characterize VEEV-RABV-G, we purified VEEV-RABV-G particles through ultracentrifugation and analyzed the protein compositions of these particles by SDS-PAGE (Fig. 1d). As expected, RABV-G protein was the only viral structural protein found in the viral particles. The morphologies of VEEV-RABV-G in BHK-21 cells during viral infection were examined by thin-section transmission electron microscopy (TEM). Abundant spherical particles around 60- to 90-nm were observed on the surface of VEEV-RABV-G infected cells compared with the typical bullet-shaped particles of RABV (Fig. 1e). Overall, our results demonstrated that VEEV-RABV-G could assembly infectious viral particles that were quite different from RABV in both shape and size.

Genetic stability is one of the essential properties for an optimal live-attenuated vaccine. Three independent VEEV-RABV-G (A, B and C) were passaged on BHK-21 cells. After 10 rounds of passage, the growth kinetic (Fig. 1f), plaque morphology (Fig. 1g) and RABV-G protein expression (Fig. 2c) were identified on BHK-21 cells. Also, RABV-G gene was confirmed by RT-PCR in viral particles from both P_0 and P_{10} passages (Fig. 2b). These results indicated that VEEV-RABV-G could continuously passage in cell lines and it possessed high genetic stability.

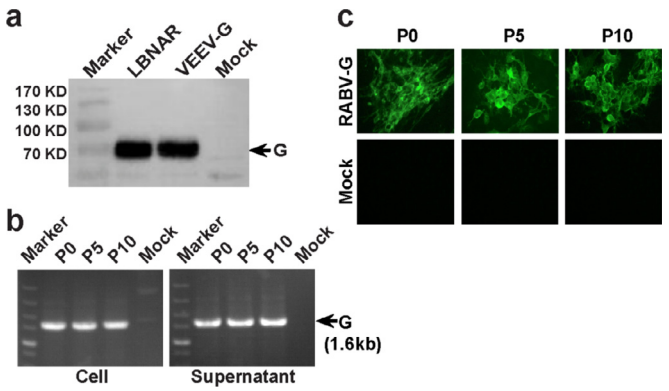

Fig. 2. Genetic stability of VEEV-RABV-G. (a) Western Blotting analysis of RABV G protein expression in cell culture from VEEV-RABV-G infected cells (b) RT-PCR analysis of viral genome stability during passage. (c) IFA analysis of G protein expression in P0, P5 and P10 VEEV-RABV-G using RABV-G murine monoclonal antibody.

3.2. VEEV-RABV-G is highly attenuated in mice

To evaluate the safety of VEEV-RABV-G vaccine candidate, we compared the pathogenicity of VEEV-RABV-G with that of RABV vaccine strains, LBNAR and LBNSE in a mouse model. To be noted, LBNAR is a recombinant strain derived from RABV vaccine strain SAD-L16 currently used to immunize wildlife in Europe; LBNSE is derived from LBNAR with mutations at amino acid positions 194 and 333 in G protein, resulting in further attenuation of virulence in adult mouse brains [26]. Groups of adult ICR mice (6-8 weeks old) were respectively inoculated intracerebrally (i.c.) with 5×10^3 FFU of VEEV-RABV-G, LBNAR or LBNSE or mock-infected with DMEM, and these mice were monitored daily for survival ratio and body weight loss. LBNAR-infected adult mice exhibited rabies signs including depression or restless behavior (score 1), posterior paresis (score 2), general paralysis (score 3) and coma (score 4) and finally died within 9 days; LBNSE-infected mice exhibited depression or restless behavior (score 1) for a few days, but finally made a recovery and survived the i.c. infection; VEEV-RABV-G-infected mice all survived (Fig. 3b). Interestingly, as shown in Fig. 3a, no differences in body weight loss were observed between VEEV-RABV-G- and mock-infected mice, while the body weight of LBNSE-infected mice was significantly decreased after 5 d.p.i.

For the further pathogenetic evaluation of VEEV-RABV-G in young animals with incomplete immune system, groups of suckling ICR mice (3-5 days old) were inoculated via i.c. route with 2×10^3 FFU of VEEV-RABV-G, LBNSE or mock infected with DMEM, respectively, and then were monitored daily for 21 days. As shown in Fig. 3d, LBNSE caused 100 % death in suckling mice at 6 d.p.i., while VEEV-RABV-G-infected mice survived the intracranial infection. Notably, no obvious clinical signs were observed in VEEV-RABV-G infected mice, though there were significant differences in body weight loss between VEEV-RABV-G and mock infected mice after 8 d.p.i (Fig. 3c).

Pathological changes of brains caused by i.c infection were then analyzed by hematoxylin and eosin (H&E) staining (Fig. 3e). Groups of adult ICR mice (6-8 weeks old) were i.c. inoculated with VEEV-RABV-G, LBNAR, LBNSE and DMEM, respectively. At 9 d.p.i., mouse brains were harvested and made into paraffin sections followed by staining with H&E. Virus-induced inflammatory tissue changes

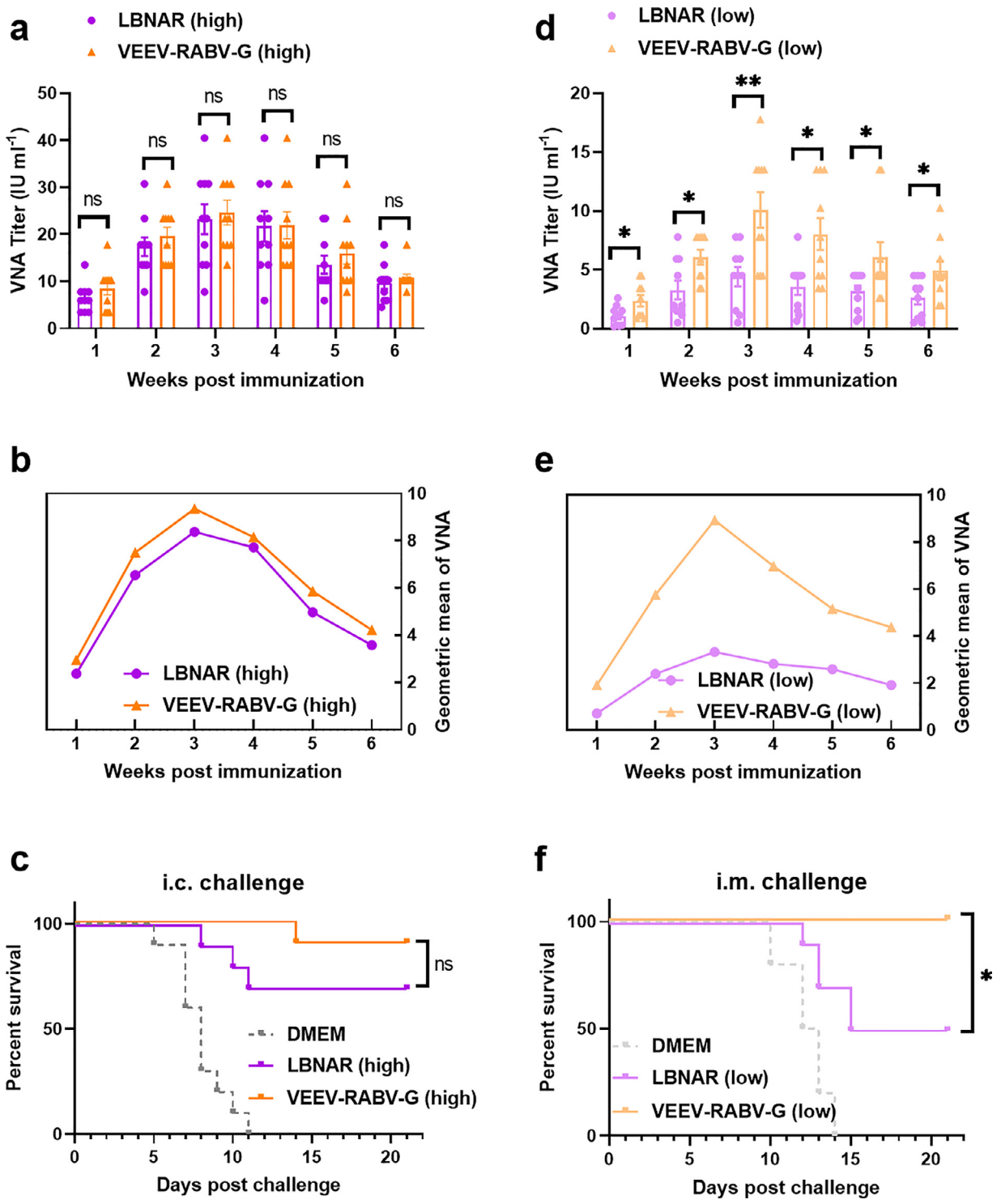

Fig. 3. Virulence of VEEV-RABV-G in adult and suckling mice. (a and b) Groups of 6-week old female ICR mice ($n = 10$ / group) were via IC. infected with 5×10^3 FFU of VEEV-RABV-G, LBNSE, LBNAR or mock-infected with 25 μl DMEM. (a) Body weight loss was then monitored daily for 15 days, and (b) mortality rates were recorded daily for 21 days. (c and d) Groups of 3-day old suckling ICR mice ($n = 15$ / group) were i.c. infected with 2×10^3 FFU of VEEV-RABV-G, LBNSE, or were mock-infected with 5 μl DMEM. (c) Body weight loss was then monitored daily for 15 days, and (d) mortality rates were recorded daily for 21 days. (e) Groups of 6-week old female ICR mice ($n = 5$ / group) were i.c. infected with 5×10^3 FFU of VEEV-RABV-G, LBNSE, LBNAR or mock-infected with 25 μl DMEM. At 9 d.p.i., sagittal sections of the mouse brain were cut and stained with H&E, and histopathological analysis of different brain regions including pons (Pons), thalamus (Thala), hippocampus (Hippo) and cerebral cortex (Cere) were performed, and the representative histological changes (scale bars, 20 μm) were presented. Black triangles indicate the pathological changes including inflammatory cuffs of blood vessels (perivascular cuffing) and/or intravascular coagulations. Data are presented as means ± SEM. Asterisks indicate significant differences between the indicated experimental groups, ** $p < 0.01$, *** $p < 0.001$ (Student's *t*-test). Yellow asterisks represents difference between VEEV-RABV G and DMEM, blue asterisks represents difference between LBNSE and DMEM, and purple asterisks represents difference between LBNAR and DMEM.

including perivascular cuffing, infiltration of inflammatory cells and neuron necrosis were observed in both LBNAR and LBNSE infected brains. In contrast, no obvious pathological changes were observed in VEEV-RABV-G infected brains, except only a very few inflammatory cells in the hippocampus region.

To further confirm neuroinflammation and neuron necrosis in virus-infected brains, brain sections were stained with pan-leukocyte marker-CD45 (Fig. 4a) and cell apoptosis marker-caspase 3 (Fig. 4c), respectively. The integrated optical density (IOD) values of positive signals representing inflammations (Fig. 4b) and nerve injuries (Fig. 4d) in brains were analyzed using ImageJ software, and the data were normalized to the IOD values of the corresponding DMEM samples. As expected, much less accumulation of CD45 positive inflammatory cells and caspase 3 positive necrotic neurons in VEEV-RABV-G-infected brains than that in LBNAR- or LBNSE-infected brains were observed.

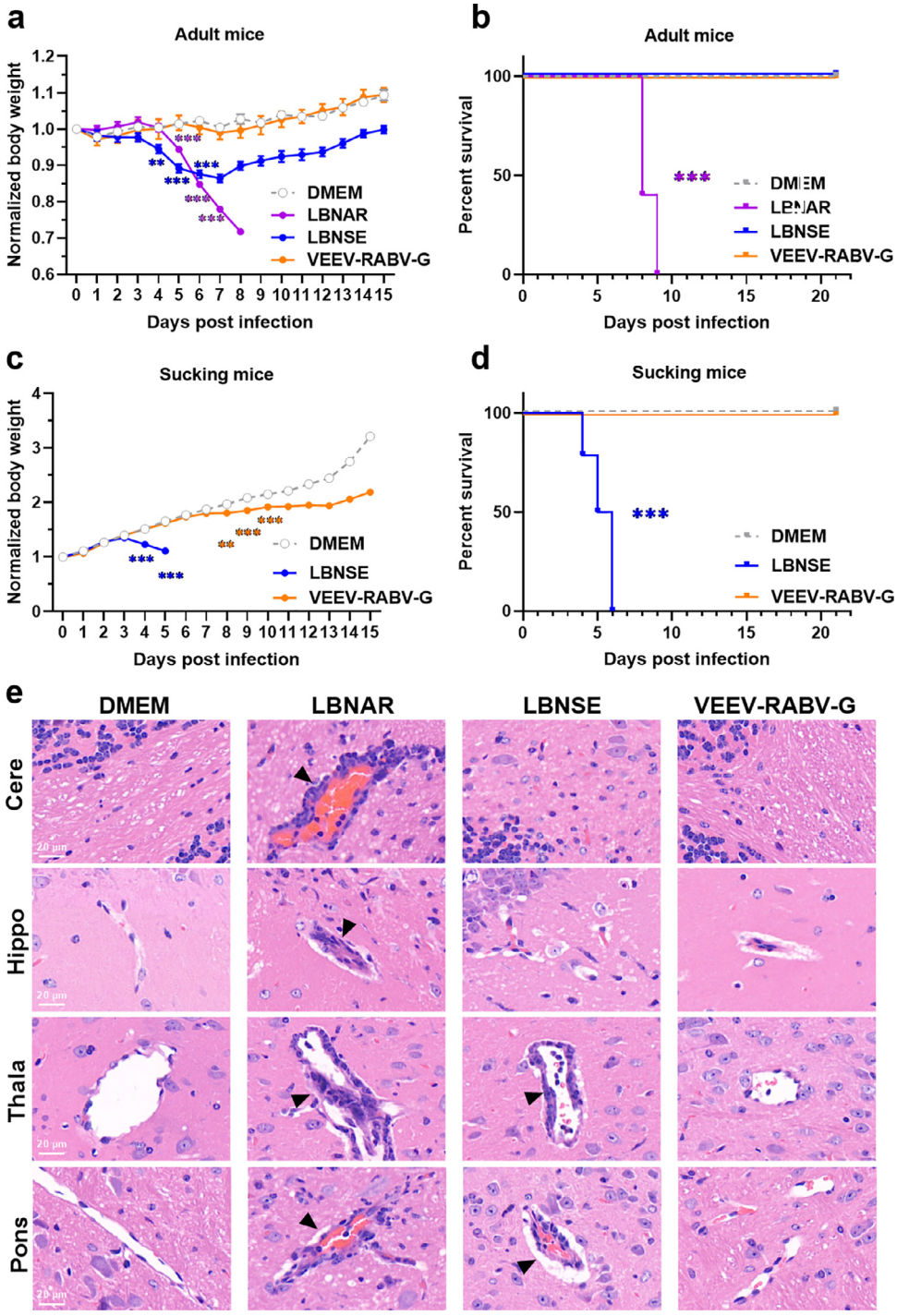

Fig. 4. Pathological changes of VEEV-RABV-G in adult mice. Groups of 6-week old female ICR mice (n = 5 / group) were i.c. infected with 5×10^3 FFU of VEEV-RABV-G, LBNSE, LBNAR or mock-infected with 25 μl DMEM. Brain sagittal sections of infected mice were cut and immunohistochemically (IHC) stained with CD45 (a) or caspase 3 antibody (c). Representative histological images at 200 × magnifications (scale bars, 200 μm) in different brain regions including pons (Pons), thalamus (Thala), hippocampus (Hippo) and cerebral cortex (Cere). Positive DAB signals (brown) representing CD45 (b) or caspase 3 (d) were analyzed by integrated optical density (IOD) of positive signals (brown, DAB) using NIH Image J software (IHC toolbox). Statistical data are presented as means ± SEM. Asterisks indicate significant differences between the indicated experimental groups, * $p < 0.05$, ** $p < 0.01$, *** $p < 0.001$.

3.3. VEEV-RABV-G provides protection against virulent RABV challenge in mice

RABV-specific VNA plays a major role in defensing against virulent RABVs. To evaluate the immunogenicity and protective efficacy of VEEV-RABV-G, three groups of ICR mice (6-8 weeks old) were i.m. immunized with 2×10^5 FFU of VEEV-RABV-G, LBNAR or mock-immunized with DMEM, VNA titers in a continuous six weeks post immunization were determined by the FAVN method [8, 20]. As shown in Fig. 5a, mathematic mean of VNA induced by VEEV-RABV-G was comparable to that induced by LBNAR. The geometric mean titer (GMT) of VNA induced by VEEV-RABV-G could reach a maximum of 23.3826 IU/ml at 3 weeks p.i., which was similar to that (20.9480 IU/ml) in LBNAR-immunized mice (Fig. 5b). At six weeks post-immunization, all mice were i.c. challenged with $50 \times LD_{50}$ CVS-24, all mice of mock group succumbed to rabies within 11 days, while 90% of the mice immunized with VEEV-RABV-G survived the lethal challenge compared with only 70% of survival rate in the LBNAR group (Fig. 5c).

Given the potential application of a vaccine candidate in the future, it is necessary to evaluate the immune efficacy and protective ability provided by low-dose VEEV-RABV-G. Three groups of ICR mice (6-8 weeks old) were via i.m. immunized with low-dose (2×10^4 FFU) of VEEV-RABV-G, LBNAR or mock- immunized with DMEM. The mice immunized with VEEV-RABV-G induced significantly higher VNA titers than the mice immunized with LBNAR (Fig. 5d). The GMT of VNA induced by low-dose VEEV-RABV-G could reach a maximum of 8.9416 IU/ml at 3 weeks p.i. compared with 3.3266 IU/ml induced by LBNAR (Fig. 5e). At 8 weeks post-immunization, all mice were i.m. challenged with $100 \times LD_{50}$ DRV-Mexico, and then the survival ratio was monitored for another 21 days. All mice of mock group succumbed to rabies within 14 days, while 100% of the mice immunized with VEEV-RABV-G were protected from the lethal challenge compared with only 50% of survival rate in LBNAR group (Fig. 5f). These results suggested that VEEV-RABV-G can induce higher VNA and provide better protection against virulent RABVs than LBNAR can do.

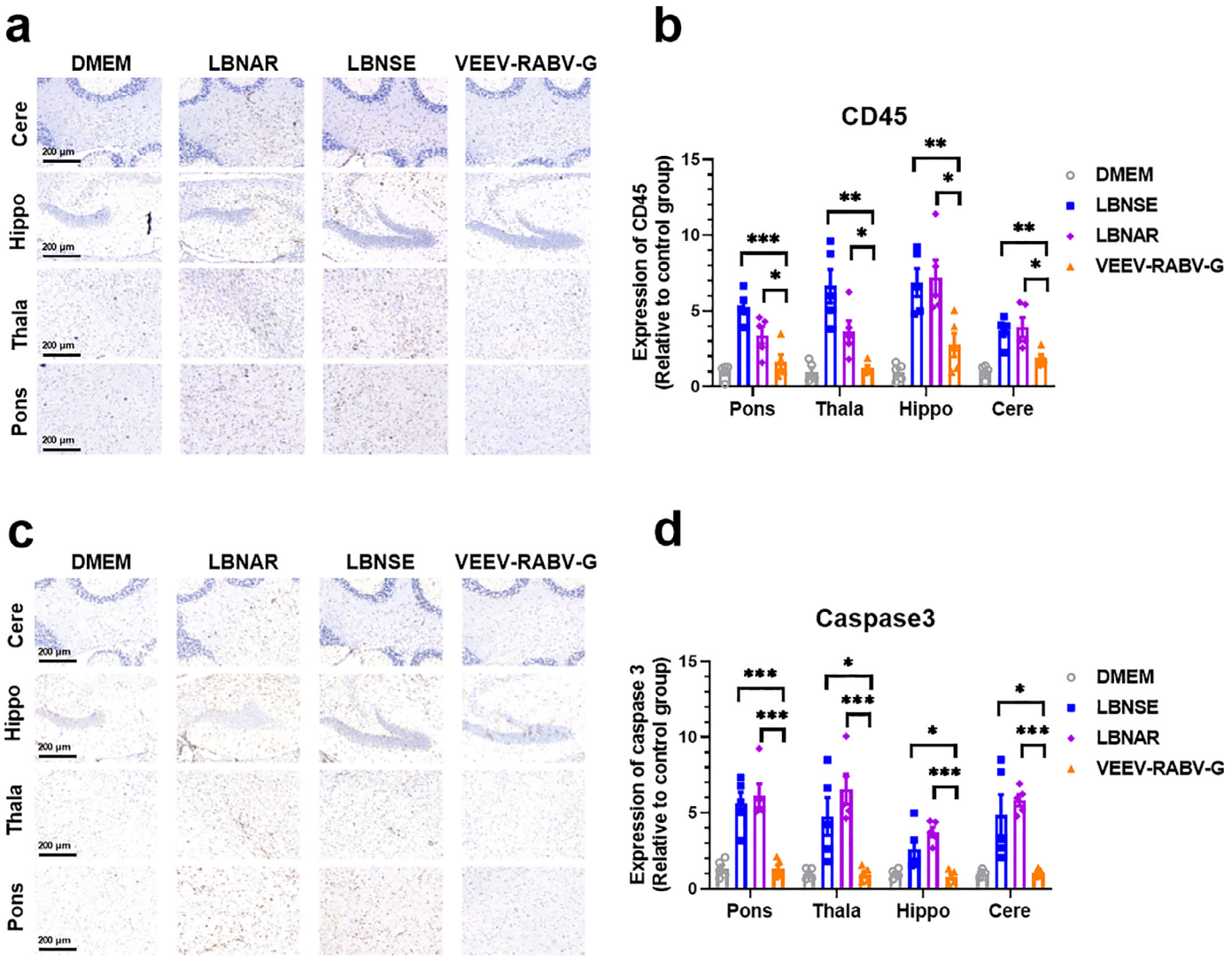

Fig. 5. The VEEV-RABV-G induces RABV-specific VNA titers and improves protection against virulent RABV. (a to c) Groups of 6-week old female ICR mice ($n = 10$ / group) were via i.m. immunized with 2×10^5 FFU of VEEV-RABV-G, LBNAR or mock-immunized with 100 μl DMEM. At the indicated time points post immunization, serum was collected from peripheral blood samples to quantify (a) VNA titers and (b) VNA GMT titers, which were determined using FAVN as described in Materials and Methods. (c) At sixth week post-immunization, all mice were i.c. challenged with $50 \times LD_{50}$ of CVS-24 virulent strain. The survival rates in different immunization groups were recorded. (d to f) Groups of 6-week-old female ICR mice ($n = 10$ / group) were i.m. immunized with 2×10^4 FFU of VEEV-RABV-G, LBNAR or mock-immunized with 100 μl DMEM. (d) VNA titers and (e) VNA GMT titers were determined. (f) At eighth week post-immunization, all mice were i.m. challenged with $100 \times LD_{50}$ of virulent strain of RABV, DRV-Mexico, and the mortality of different immunization groups were recorded. Statistical data are presented as means ± SEM, and asterisks indicate significant differences between the indicated experimental groups, $^*p<0.05$, $^{**}p<0.01$, ns means "not significant" (Survival curves were analyzed by *log-rank* test, other data was analyzed by student's *t*-test).

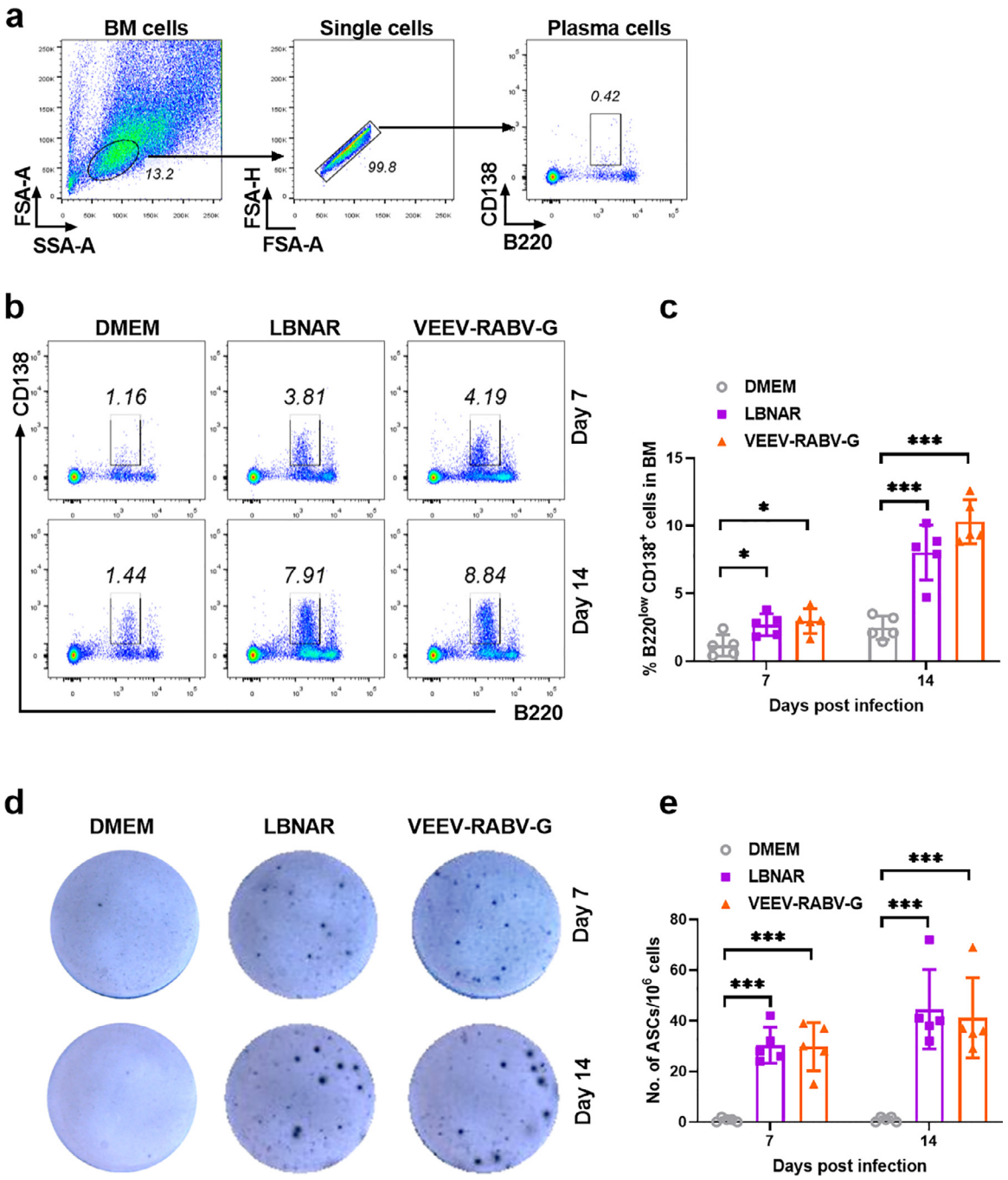

Fig. 6. The VEEV-RABV-G induce the generation of PCs and RABV-specific ASCs. Three groups of C57BL/6 mice (n = 5 / group) were i.m. inoculated with 100 μl of DMEM or 2×10^4 FFU VEEV-RABV-G or 2×10^4 FFU LBNAR. The bone marrow (BM) of mice was collected at 7 and 14 d.p.i. After removing red blood cells with ACK lysis buffer, the single-cell suspensions were prepared, stained and analyzed the proportion of $B220^{low}CD138^+$ plasma cells by flow cytometry. (a) Representative gating strategy for the detection of PCs in BM cells using flow cytometry. (b) Representative flow cytometric plots of PCs from the three groups. (c) Statistical results of PCs among BM cells are presented. The inguinal LNs were collected post-immunization at 7 and 14 days, and single-cell suspensions of the inguinal LNs were prepared for analysis of RABV-specific ASCs by ELISpot ($n = 5$ / group). Representative sections are shown in (d) and numbers of ASCs are shown in (e). Data are presented as means ± SEM. Asterisks indicate significant differences between the indicated experimental groups, * $p<0.05$, *** $p < 0.001$ (Student's *t*-test).

3.4. VEEV-RABV-G induces robust generation of antibody-secreting cells

Germinal centers (GC) are the critical sites for the generation and selection of B cells that produce high-affinity antibodies [27]. After extensive selection, GC B cells finally differentiate into plasma cells (PCs) residing in BM and ASCs residing in LNs [28]. In order to evaluate the generation of these immune cells post VEEV-RABV-G vaccination, three groups of C57BL/6 mice (6-8 weeks old) were i.m. immunized with VEEV-RABV-G, LBNAR and DMEM, respectively. At 7 and 14 d.p.i., PCs within BMs of immunized mice were collected and analyzed by flow cytometry. The gating strategy and representative flow cytometric plots for PCs ($B220^{low}$ $CD138^+$) are shown in Fig. 6a and 6b, respectively. Mice immunized with VEEV-RABV-G or LBNAR generated significantly more PCs in the BM than those immunized with DMEM at both 7 and 14 days p.i. (Fig. 6c). Furthermore, the generation of RABV-specific ASCs in inguinal lymph nodes was evaluated by ELISpot assay. As expected, RABV-specific ASCs in VEEV-RABV-G or LBNAR immunized mice were obviously more than those in

DMEM immunized mice (Fig. 6d and 6e). Together, these results suggest that VEEV-RABV-G could induce robust generation of PCs and RABV-specific ASCs.

4. Discussion

The alphaviruses from the *Togaviridae* family are positive-strand RNA viruses including Sindbis virus (SINV), Semliki Forest virus (SFV) and Venezuelan equine encephalitis virus (VEEV), which are widely used as vaccine vectors for many infectious diseases [29]. The 5′ end of the alphavirus genome encodes four nonstructural proteins for transcription and replication of the RNA genome and the structural proteins are expressed from a subgenomic RNA transcribed from the 26S subgenomic promoter immediately downstream of the nonstructural proteins [30]. Alphavirus vectors for gene delivery are known as replicons by replacing viral structural proteins with the gene of interest for antigens expression [31]. Normally, the alphavirus replicons may be packaged into virus replicon particles (VRPs) by providing the alphavirus capsid and envelope proteins *in trans* for gene delivery [29]. SINV and SFV vectors have been engineered as VRPs or nucleic acid vaccine delivering RABV glycoprotein (RABV G) to induce protective immune responses [32-35]. In this study, a novel VEEV replicon-derived, self-propagating replicon particles (PRPs) expressing RABV-G protein, designated as VEEV-RABV-G, was developed as a live attenuated rabies vaccine. Different with the previous constructs [32-35], VEEV-RABV-G is self-replicative and is able to efficiently propagate to high titers in cell culture without any other structural proteins provided *in trans* (Fig. 1f).

Similar strategies have been used to construct the hybrid SFV/VSV PRPs (also called SFVG) by replacing SFV structural protein with the glycoprotein (G) of vesicular stomatitis virus (VSV) [36-38]. It was proposed that vesiculation of plasma membrane is the possible mechanism by which such hybrid PRPs are formed [36]. Specifically, the light bulb shaped SFV replication complexes (spherules) are formed at the plasma membrane during the replication of SFV replicon RNA that are followed by the budding of infectious membrane-enveloped particles containing VSV G protein and the SFV replicon. It has been demonstrated that fusion activity of VSV-G is essential for this process. As both RABV and VSV are the members of *Rhabdoviridae* family, we hypothesize that VEEV-RABV-G might follow the same mechanism for particle assembly. With RABV-G as the single viral structural protein displaying on the surface (Fig. 1d and 2a), VEEV-RABV-G particles shared similar antigenicity to RABV and thus exhibited the ability to induce protective immunity against rabies (Fig. 4-6).

ELISpot assay was performed to assess the generation of ASCs in the inguinal LNs. It showed that RABV-specific ASCs in mice immunized with VEEV-RABV-G were comparable to those in mice after vaccination with LBNAR, which also indicated that the total antibody levels by these two vaccines were comparable (Fig. 6). Interestingly, VEEV-RABV-G induced a higher level of VNA than LBNAR did when mice were immunized with low dose of vaccines (2×10^4 FFU), contributing to enhanced protection in mice (Fig. 5d-5f). As we know, among the antibodies produced by ASCs, only a subset of these antibodies, namely VNA acts as a critical component to block virus infection [39], but it still needs further investigation about the detailed mechanism by which VEEV-RABV-G vaccine induced such prominent VNA responses in mice.

Safety issues are always the major concern for the development of RABV LAVs. For the LAVs derived from blind passage of virulent strains, such as SAD Bern, SAD B19 and SAG2 that are currently used for wildlife vaccination, their possible reversion to virulence has been the critical limitation for their further utilization in pets, especially in human [40, 41]. Several replicating viral vectored vaccines expressing RABV G protein have been developed, including vaccinia virus, adenovirus, pox virus, New castle virus and parainfluenza virus 5 etc. [12, 13, 42-45], but there are still some vaccine-associated adverse events, especially in the immune-compromised individuals reported during their utilization. It has been reported that two people displayed intensive skin inflammation and systemic vaccinia infection after they had contacted closely with the dogs vaccinated with vaccinia virus based RABV vaccine [46]. In contrast, VEEV-RABV-G not only exhibited a satisfactory genetic stability (Fig. 1f, 1g and Fig. 2), but also was highly attenuated with gradually increased body weight, a 100% survival rate and no obvious brain pathology in mice (Fig. 3 and 4). What's more, it was avirulent in suckling mice even through i. c. infection (Fig. 3c and 3d), indicating its safety as a novel LAV candidate.

In summary, the VEEV-RABV-G PRPs are proved to be safe and effective in mouse model, and can be a promising RABV vaccine candidate for human and domestic animal use. In addition, the PRPs may represent a universal strategy for the development of other vaccines like the newly emerging COVID-19 vaccine, due to the infectious, self-amplifying capabilities.

Acknowledgement

We are grateful to the Core Facility and Technical Support, Wuhan Institute of Virology, for their help with producing TEM micrographs.

Funding Sources

This work was supported by the National Key Research and Development Program of China (2016YFD0500400). The funders had no role in study design, data collection and interpretation, or the decision to submit the work for publication.

Declaration of Interests

The authors declare no competing interests. Dr. Bo Zhang, Dr. Ling Zhao, Ms. Yan-Nan Zhang, Mr. Chen Chen have a patent pending to Chinese Office of Patents, which is relevant to this work.

Author Contributions

BZ and LZ conceived this study. BZ, YNZ, CC and LZ, drafted the manuscript. YNZ developed VEEV-RABV-G construct and performed virological experiments. CC, YNZ and CGZ performed all animal study and CC conducted data analysis. CLD, NL· and ZW respectively contributed to Western blotting, RT-PCR or IFA assay for genetic stability assay of VEEV-RABV-G.

References

[1] Robardet E, Bosnjak D, Englund L, Martin PR, Cliquet F. Zero Endemic Cases of Wildlife Rabies (Classical Rabies Virus, RABV) in the European Union by 2020: An Achievable Goal. Tropical medicine and infectious disease 2019;4(4).
[2] Faber M, Li J, Kean RB, Hooper DC, Alugupalli KR, Dietzschold B. Effective preexposure and postexposure prophylaxis of rabies with a highly attenuated recombinant rabies virus. Proceedings of the National Academy of Sciences of the United States of America 2009;106(27):11300–5.
[3] Timiryasova TM, Luo P, Zheng L, Singer A, Zedar R, Garg S, et al. Rapid fluorescent focus inhibition test optimization and validation: Improved detection of neutralizing antibodies to rabies virus. Journal of immunological methods 2019.
[4] Bonnaud EM, Troupin C, Dacheux L, Holmes EC, Monchatre-Leroy E, Tanguy M, et al. Comparison of intra- and inter-host genetic diversity in rabies virus during experimental cross-species transmission. PLoS pathogens 2019;15(6):e1007799.
[5] Giesen A, Gniel D, Malerczyk C. 30 Years of rabies vaccination with Rabipur: a summary of clinical data and global experience. Expert review of vaccines 2015;14(3):351–67.
[6] RabAvert: new human rabies vaccine approved in the United States. International journal of trauma nursing 1998;4(2):58–60.
[7] Zhu S, Guo C. Rabies Control and Treatment: From Prophylaxis to Strategies with Curative Potential. Viruses 2016;8(11).
[8] Wang Z, Li M, Zhou M, Zhang Y, Yang J, Cao Y, et al. A Novel Rabies Vaccine Expressing CXCL13 Enhances Humoral Immunity by Recruiting both T Follicular Helper and Germinal Center B Cells. Journal of virology 2017;91(3).

[9] Li Y, Zhou M, Luo Z, Zhang Y, Cui M, Chen H, et al. Overexpression of Interleukin-7 Extends the Humoral Immune Response Induced by Rabies Vaccination. Journal of virology 2017;91(7).
[10] Huang J, Zhang Y, Huang Y, Gnanadurai CW, Zhou M, Zhao L, et al. The ectodomain of rabies virus glycoprotein determines dendritic cell activation. Antiviral research 2017;141:1–6.
[11] da Fontoura Budaszewski R, Hudacek A, Sawatsky B, Kramer B, Yin X, Schnell MJ, et al. Inactivated Recombinant Rabies Viruses Displaying Canine Distemper Virus Glycoproteins Induce Protective Immunity against Both Pathogens. Journal of virology 2017;91(8).
[12] Kieny MP, Lathe R, Drillien R, Spehner D, Skory S, Schmitt D, et al. Expression of rabies virus glycoprotein from a recombinant vaccinia virus. Nature 1984;312 (5990):163–6.
[13] Ge J, Wang X, Tao L, Wen Z, Feng N, Yang S, et al. Newcastle disease virus-vectored rabies vaccine is safe, highly immunogenic, and provides long-lasting protection in dogs and cats. Journal of virology 2011;85(16):8241–52.
[14] Wiktor TJ, Macfarlan RI, Reagan KJ, Dietzschold B, Curtis PJ, Wunner WH, et al. Protection from rabies by a vaccinia virus recombinant containing the rabies virus glycoprotein gene. Proceedings of the National Academy of Sciences of the United States of America 1984;81(22):7194–8.
[15] Weyer J, Rupprecht CE, Nel LH. Poxvirus-vectored vaccines for rabies—a review. Vaccine 2009;27(51):7198–201.
[16] Li Z, Wang J, Yuan D, Wang S, Sun J, Yi B, et al. A recombinant canine distemper virus expressing a modified rabies virus glycoprotein induces immune responses in mice. Virus genes 2015;50(3):434–41.
[17] Yarosh OK, Wandeler AI, Graham FL, Campbell JB, Prevec L. Human adenovirus type 5 vectors expressing rabies glycoprotein. Vaccine 1996;14(13):1257–64.
[18] Zhang S, Liu Y, Fooks AR, Zhang F, Hu R. Oral vaccination of dogs (Canis familiaris) with baits containing the recombinant rabies-canine adenovirus type-2 vaccine confers long-lasting immunity against rabies. Vaccine 2008;26(3):345–50.
[19] Osakada F, Callaway EM. Design and generation of recombinant rabies virus vectors. Nature protocols 2013;8(8):1583–601.
[20] Zhao L, Toriumi H, Wang HL, Kuang Y, Guo XF, Morimoto K, et al. Expression of MIP-1 alpha (CCL3) by a Recombinant Rabies Virus Enhances Its Immunogenicity by Inducing Innate Immunity and Recruiting Dendritic Cells and B Cells. Journal of virology 2010;84(18):9642–8.
[21] Wen YJ, Wang HL, Wu H, Yang FH, Tripp RA, Hogan RJ, et al. Rabies Virus Expressing Dendritic Cell-Activating Molecules Enhances the Innate and Adaptive Immune Response to Vaccination. Journal of virology 2011;85(4):1634–44.
[22] Yu FL, Zhang GQ, Zhong XF, Han N, Song YF, Zhao L, et al. Comparison of complete genome sequences of dog rabies viruses isolated from China and Mexico reveals key amino acid changes that may be associated with virus replication and virulence. Archives of virology 2014;159(7):1593–601.
[23] Dietzschold B, Morimoto K, Hooper DC, Smith JS, Rupprecht CE, Koprowski H. Genotypic and phenotypic diversity of rabies virus variants involved in human rabies: Implications for postexposure prophylaxis. J Human Virol 2000;3(1):50–7.
[24] Zhang YN, Deng CL, Li JQ, Li N, Zhang QY, Ye HQ, et al. Infectious Chikungunya Virus (CHIKV) with a Complete Capsid Deletion: a New Approach for a CHIKV Vaccine. J Virol 2019;93(15).
[25] Luo Z, Li Y, Zhou M, Lv L, Wu Q, Chen C, et al. Toll-Like Receptor 7 Enhances Rabies Virus-Induced Humoral Immunity by Facilitating the Formation of Germinal Centers. Frontiers in immunology 2019;10:429.
[26] Wen Y, Wang H, Wu H, Yang F, Tripp RA, Hogan RJ, et al. Rabies virus expressing dendritic cell-activating molecules enhances the innate and adaptive immune response to vaccination. Journal of virology 2011;85(4):1634–44.
[27] Haberman AM, Gonzalez DG, Wong P, Zhang TT, Kerfoot SM. Germinal center B cell initiation, GC maturation, and the coevolution of its stromal cell niches. Immunol Rev 2019;288(1):10–27.
[28] Ise W, Kurosaki T. Plasma cell differentiation during the germinal center reaction. Immunol Rev 2019;288(1):64–74.
[29] Perri S, Greer CE, Thudium K, Doe B, Legg H, Liu H, et al. An alphavirus replicon particle chimera derived from venezuelan equine encephalitis and sindbis viruses is a potent gene-based vaccine delivery vector. Journal of virology 2003;77 (19):10394–403.
[30] Jurgens CK, Young KR, Madden VJ, Johnson PR, Johnston RE. A novel self-replicating chimeric lentivirus-like particle. J Virol 2012;86(1):246–61.
[31] Polo JM, Belli BA, Driver DA, Frolov I, Sherrill S, Hariharan MJ, et al. Stable alphavirus packaging cell lines for Sindbis virus and Semliki Forest virus-derived vectors. Proc Natl Acad Sci U S A 1999;96(8):4598–603.
[32] Suarez-Patino SF, Bernardino TC, Nunez EGF, Astray RM, Pereira CA, Soares HR, et al. Semliki Forest Virus replicon particles production in serum-free medium BHK-21 cell cultures and their use to express different proteins. Cytotechnology 2019;71(5):949–62.
[33] Astray RM, Ventini DC, Boldorini VL, Silva FG, Rocca MP, Pereira CA. Rabies virus glycoprotein and immune response pattern using recombinant protein or recombinant RNA viral vectors. Vaccine 2014;32(24):2829–32.
[34] Gupta PK, Dahiya SS, Kumar P, Rai A, Patel CL, Sonwane AA, et al. Sindbis virus replicon-based DNA vaccine encoding Rabies virus glycoprotein elicits specific humoral and cellular immune response in dogs. Acta Virol 2009;53(2):83–8.
[35] Saxena S, Dahiya SS, Sonwane AA, Patel CL, Saini M, Rai A, et al. A sindbis virus replicon-based DNA vaccine encoding the rabies virus glycoprotein elicits immune responses and complete protection in mice from lethal challenge. Vaccine 2008;26(51):6592–601.
[36] Rolls MM, Webster P, Balba NH, Rose JK. Novel infectious particles generated by expression of the vesicular stomatitis virus glycoprotein from a self-replicating RNA. Cell 1994;79(3):497–506.
[37] Rose NF, Publicover J, Chattopadhyay A, Rose JK. Hybrid alphavirus-rhabdovirus propagating replicon particles are versatile and potent vaccine vectors. Proceedings of the National Academy of Sciences of the United States of America 2008;105(15):5839–43.
[38] Rose NF, Buonocore L, Schell JB, Chattopadhyay A, Bahl K, Liu X, et al. In vitro evolution of high-titer, virus-like vesicles containing a single structural protein. Proceedings of the National Academy of Sciences of the United States of America 2014;111(47):16866–71.
[39] Rhorer J, Ambrose CS, Dickinson S, Hamilton H, Oleka NA, Malinoski FJ, et al. Efficacy of live attenuated influenza vaccine in children: A meta-analysis of nine randomized clinical trials. Vaccine 2009;27(7):1101–10.
[40] Mähl P, Cliquet F, Guiot A-L, Niin E, Fournials E, Saint-Jean N, et al. Twenty year experience of the oral rabies vaccine SAG2 in wildlife: a global review. Veterinary research 2014;45(1) 77-.
[41] Hsu AP, Tseng CH, Barrat J, Lee SH, Shih YH, Wasniewski M, et al. Safety, efficacy and immunogenicity evaluation of the SAG2 oral rabies vaccine in Formosan ferret badgers. PloS one 2017;12(10):e0184831.
[42] Amann R, Rohde J, Wulle U, Conlee D, Raue R, Martinon O, et al. A New Rabies Vaccine Based on a Recombinant Orf Virus (Parapoxvirus) Expressing the Rabies Virus Glycoprotein. Journal of virology 2013;87(3):1618–30.
[43] Chen ZH, Zhou M, Gao XD, Zhang GQ, Ren GP, Gnanadurai CW, et al. A Novel Rabies Vaccine Based on a Recombinant Parainfluenza Virus 5 Expressing Rabies Virus Glycoprotein. Journal of virology 2013;87(6):2986–93.
[44] Blancou J, Kieny MP, Lathe R, Lecocq JP, Pastoret PP, Soulebot JP, et al. Oral vaccination of the fox against rabies using a live recombinant vaccinia virus. Nature 1986;322(6077):373–5.
[45] Tims T, Briggs DJ, Davis RD, Moore SM, Xiang Z, Ertl HC, et al. Adult dogs receiving a rabies booster dose with a recombinant adenovirus expressing rabies virus glycoprotein develop high titers of neutralizing antibodies. Vaccine 2000;18 (25):2804–7.
[46] Rupprecht CE, Blass L, Smith K, Orciari LA, Niezgoda M, Whitfield SG, et al. Human infection due to recombinant vaccinia-rabies glycoprotein virus. The New England journal of medicine 2001;345(8):582–6.